Response function of the magnetic spectrometer PRISMA

D. Montanari, E. Farnea, S. Leoni, G. Pollarolo, L. Corradi, G. Benzoni, A. Gadea, E. Fioretto, A. Latina, G. Montagnoli, F. Scarlassara, A.M. Stefanini and S. Szilner

THE EUROPEAN
PHYSICAL JOURNAL A

Special Article – Tools for Experiment and Theory

Response function of the magnetic spectrometer PRISMA

D. Montanari[1,2], E. Farnea[3], S. Leoni[1,2,a], G. Pollarolo[4], L. Corradi[5], G. Benzoni[2], A. Gadea[5,6], E. Fioretto[5], A. Latina[4], G. Montagnoli[7,3], F. Scarlassara[7,3], A.M. Stefanini[5], and S. Szilner[8]

1 Dipartimento di Fisica, Università di Milano, Milano, Italy
2 INFN, Sezione di Milano, Milano, Italy
3 INFN, Sezione di Padova, Padova, Italy
4 Dipartimento di Fisica Teorica, Università di Torino and INFN Sezione di Torino, Torino, Italy
5 Laboratori Nazionali di Legnaro, INFN, Legnaro, Italy
6 IFIC, CSIC-University of Valencia, Spain
7 Dipartimento di Fisica, Università di Padova, Padova, Italy
8 Ruđer Bošković Institute, Zagreb, Croatia

Abstract. The response function of the magnetic spectrometer PRISMA is studied via a Monte Carlo simulation that employs a ray tracing code to determine the trajectories of individual rays through the electromagnetic fields. The calculated response is tested on angular and energy distributions provided by theoretical calculations for the ^{48}Ca + ^{64}Ni multinucleon transfer reaction and applied to the corresponding experimental data.

1 Introduction

Magnetic spectrometers, for both light- and heavy-ion reactions, have been built and operated since many decades with solid angles in the range 3–10 msr. More recently, a new generation of magnetic spectrometers has been developed, reaching solid angles of $\simeq 100$ msr [1–3]. With this very large acceptance, it becomes unfeasible to use complex magnetic elements to correct for the ion optical aberrations. These corrections are very relevant in the study of grazing collisions where several nuclei are produced in a wide energy and angular range and with cross sections spanning orders of magnitude.

To overcome the above difficulties, the adopted solution is to simplify the magnetic element configuration and to apply the concept of trajectory reconstruction. This can be done by using a detector system which, besides nuclear charge, energy and timing, provides the necessary position information along the ion path. These ideas, "simple" magnetic configuration and an event-by-event reconstruction of the ion trajectory, have been adopted for the large solid-angle spectrometer PRISMA of Legnaro National Laboratory of INFN (Italy) [1].

PRISMA is one of the largest acceptance magnetic spectrometer currently operating. It has been coupled to the large gamma array CLARA [4], and it is now used in the first phase of measurements with the European array AGATA [5], which is among the most advanced array for

gamma spectroscopy. As a consequence, a detailed knowledge of the performances of PRISMA, both in terms of transmission and trajectory reconstruction, is important for reaction and nuclear-structure studies.

The understanding of the reaction mechanism depends strongly on the knowledge of absolute cross sections which requires a correct treatment of the measured yields that may be strongly affected by the transmission, especially at the edge of the spectrometer. Therefore, the response of the spectrometer has to be extracted via a simulation of ion trajectories, taking into account the kinematics of the reaction and the geometry of the magnetic elements and detectors [6].

In this paper we present a study of the response of PRISMA via a Monte Carlo simulation of the ion trajectories. The validity of the extracted response has been tested by using differential cross sections provided by the semiclassical model GRAZING [7] and by the analysis of the angular distribution of the elastic scattering and one-particle transfer channels in the ^{48}Ca on ^{64}Ni reaction at ≈ 6 MeV/A [8,9]. In addition, the quality of the trajectory reconstruction has been confirmed by the Doppler correction of γ-rays measured in coincidence with PRISMA by the γ array CLARA [4].

2 The PRISMA spectrometer

The configuration of the PRISMA spectrometer and its detector system have been described in refs. [1,10,11].
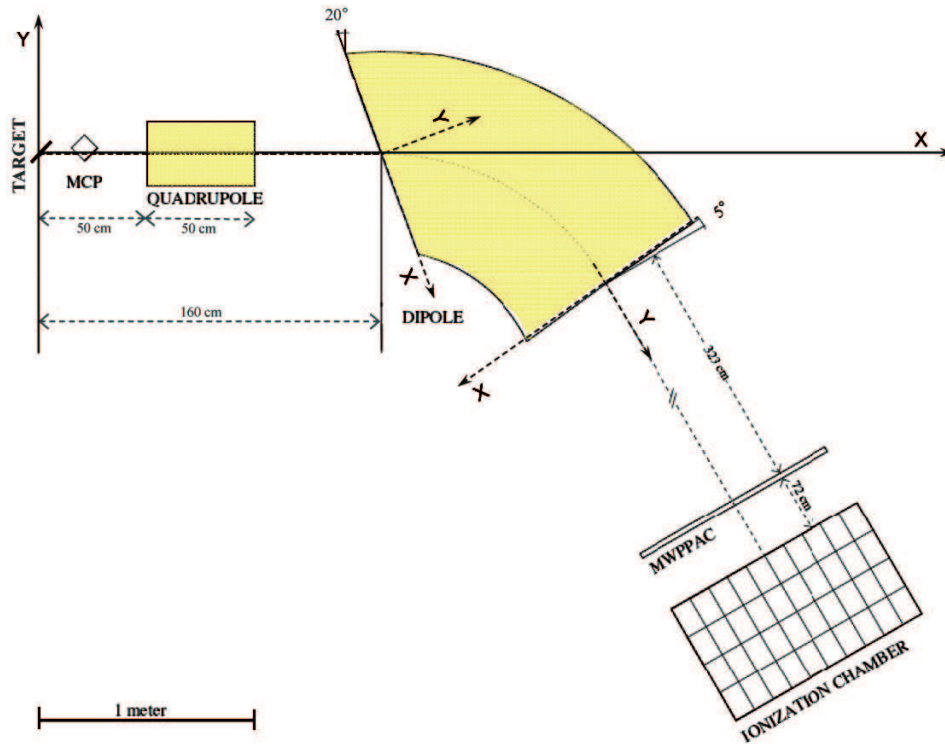
a e-mail: silvia.leoni@mi.infn.it

Fig. 1. Schematic view of the PRISMA magnetic spectrometer. The shaded regions indicate the quadrupole and dipole magnetic elements. The various reference frames relevant for the simulation calculation of the ion transport discussed in sect. 3 are also given.

Here we briefly remind the most important parameters, relevant for the reconstruction of ion trajectories.

The main characteristics of PRISMA are its solid angle of $\simeq 80\,\mathrm{msr}$ (corresponding to a geometrical acceptance of $\pm 6°$ in the horizontal and $\pm 11°$ in the vertical directions), a momentum acceptance of $\pm 10\%$ and a dispersion of $\simeq 4\,\mathrm{cm}$ per percent in momentum. The magnetic elements are a quadrupole singlet (Q), placed at $\simeq 50\,\mathrm{cm}$ from the target, and a dipole (D) with $60°$ bending angle and $1.2\,\mathrm{m}$ curvature radius. The entrance effective field boundary of the dipole, placed $60\,\mathrm{cm}$ downstream of the quadrupole, forms an angle of $-20°$ and $+5°$ at its entrance and exit, respectively. A schematic view is given in fig. 1, where we also show the reference frames used in the simulation of the trajectories.

Because of its large acceptance and its minimum number of magnetic elements PRISMA does not have a well-defined focus and the mass and charge identification are obtained after the reconstruction of the trajectory. For this purpose one needs a detection system providing two-dimensional position information at the entrance and exit of the spectrometer and time-of-flight (TOF).

The entrance detector is based on a two-dimensional position-sensitive micro-channel plate (MCP), giving a start signal for TOF (with subnanosecond resolution) and X_{MCP}, Y_{MCP} signals (with 1 mm resolutions) [10]. Ions pass through the optical elements of the spectrometer and after a path of $\simeq 6.5\,\mathrm{m}$, enter the focal plane detector [11]. This consists of an array of parallel plates of multiwire-

type (MWPPAC), providing a stop signal for TOF and X_{FOC}, Y_{FOC} position signals (with 1 mm resolutions) followed by an array of transverse field multiparametric ionization chambers (IC), giving ΔE and total energy E signals.

3 Monte Carlo simulation of the PRISMA response

For the simulation of the PRISMA response, described in this section, we remind that the motion of a particle of charge q and mass m in the spectrometer is determined by the Newtonian equation

$$\frac{\mathrm{d}}{\mathrm{d}t}m\mathbf{v} = q\mathbf{v} \times (\mathbf{B}_Q + \mathbf{B}_D) \tag{1}$$

being $\mathbf{v}$ the velocity of the ion and $\mathbf{B}_Q$ and $\mathbf{B}_D$ the magnetic fields of the quadrupole and dipole, respectively. The above equation is reduced to a system of first-order differential equations whose solution is obtained by using a Runge-Kutta algorithm of the fourth order with an adaptive step size to keep the desired accuracy. In the simulation the energy loss in the different parts of the focal plane detectors (mylar windows and gas of the MWPPAC and IC) is also taken into account [12].

Since we do not have the three-dimensional maps of the dipole and quadrupole magnetic fields we had to calculate them. The dipole magnetic field, in the entrance
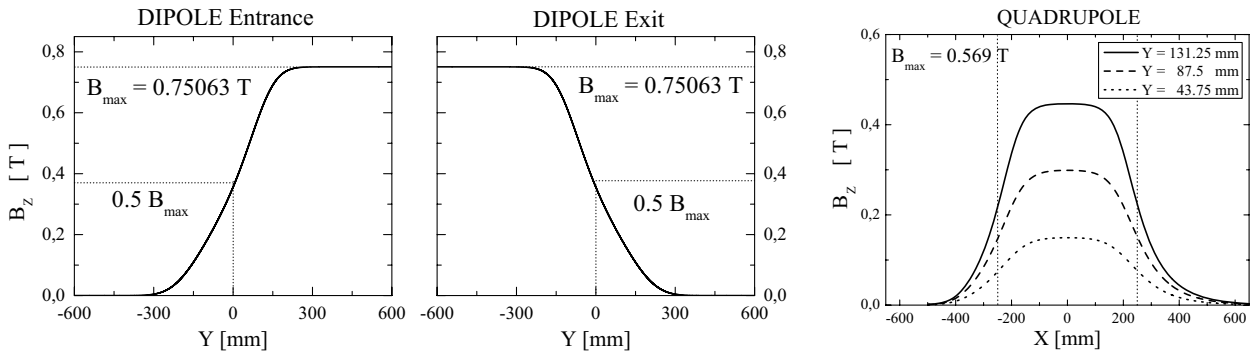
Fig. 2. Dipole and quadrupole field profiles. The dipole field profile (B_Z) is shown as a function of the transverse coordinate (Y) at the entrance and exit windows, in the fringing field region. $Y = 0$ corresponds to the entrance and exit windows of the magnet (see also fig. 1). The quadrupole field profile (B_Z) is shown at various distances from the central axis. The dotted lines at $X = \pm 250$ mm correspond to the entrance and exit windows. What look like full lines are the fields as measured by the DANFYSIK scaled for the present setting. They cover our calculated profiles.

and exit fringing field region, has been calculated from the map provided by the DANFYSIK [13] on the medium plane, by using the Maxwell equations and by expanding the field up to the fourth-order term. To calculate the field of the quadrupole element we introduced a magnetic potential that satisfies the Laplace equation. This equation has been solved by using an over-relaxation algorithm, on a three-dimensional lattice, of 1 cm size in all three directions, that is big enough to contain the full magnet. The three components of the magnetic field on the magnet poles have been calculated from the expression of the magnetic potential for a perfect quadrupole. The calculated z-component of the magnetic field has been found to agree very well with the map provided by the DANFYSIK on the medium plane. We use these calculated magnetic fields to estimate, via a linear interpolation, the force that at time t and position $\mathbf{r}(t)$ acts on the ion that is moving through the spectrometer. Figure 2 shows on the left (right) the dipole (quadrupole) field profiles corresponding to the magnetic settings used in the ^{48}Ca on ^{64}Ni reaction, lately discussed.

To calculate the response function of the spectrometer we simulate a real experiment where the initial distribution of scattered events is known. The procedure employs a ray tracing code which uses numerical integrators to determine the trajectories of individual rays through the electromagnetic fields. With our ray tracing code we produce a data file containing all the parameters detected with PRISMA; this file is then sorted with the same code used to analyze the experimental data. In the sorting code the trajectory is considered to be planar and developing in the medium plane. The trajectory, in the sorting algorithm, consists of several segments, these are linear outside the magnetic elements, hyperbolic inside the quadrupole and circular inside the dipole, the parameters defining the different segments are fitted to provide a continuous (with its first derivative) line thus allowing an estimation of the distance covered by the ion. This approximation has been carefully checked in the simulation and gives at most a 2% error in the evaluation of the length of the trajectory

allowing a sufficient resolution in mass and velocity of the ion.

The calculations are done for the reaction ^{48}Ca + ^{64}Ni at $E_{lab} = 270$ MeV, which has been recently performed for the study of elastic, inelastic and transfer reactions [8,9]. In this reaction most of the transfer yield is close to the grazing angle $\theta_{lab} = 20°$, where PRISMA was set. At this scattering angle the elastically scattered ^{48}Ca ions have an energy of ~ 250 MeV and the transfer products span an energy range of about 50 MeV.

The calculation of the response function starts by generating a distribution that is uniform in energy and isotropic in angle, covering the energy range between 150 and 400 MeV and the angular range $\theta_{lab} = 10°$–$40°$ and $\phi_{lab} = -40°$–$40°$ (see fig. 3(a)). This distribution is then transported to the focal plane by the ray tracing code outlined above, using the magnetic-field settings of the experiment (*i.e.*, $B_{max} = 0.75063$ T and 0.569 T for the dipole and quadrupole magnet, respectively). The angular range is slightly larger than the acceptance of PRISMA which is defined by the entrance area of the quadrupole. The energy range corresponds to the momentum acceptance of the spectrometer for ^{48}Ca ions, wider than the one covered by the reaction.

The ions emerge from the target with different charge states whose probability distribution follows the semi-empirical formula given in refs. [14,15]. By using in the simulation the experimental values of the quadrupole and dipole magnetic fields, we obtain the charge state distributions depicted in fig. 4 (upper panel) as a function of X_{MCP} and X_{FOC} horizontal coordinates of the entrance and focal plane detectors. To have as a reference those events which are not affected by the quadrupole field we cut the two-dimensional matrix along the central coordinate $X_{MCP} = 0$. This cut is shown on the lower panel of fig. 4. The comparison with the experiment (shown in the same figure) has to be intended as only qualitative since the calculated charge state distribution is obtained by using a uniform distribution in energy and angle. We have to warn the reader that the charge state distribution
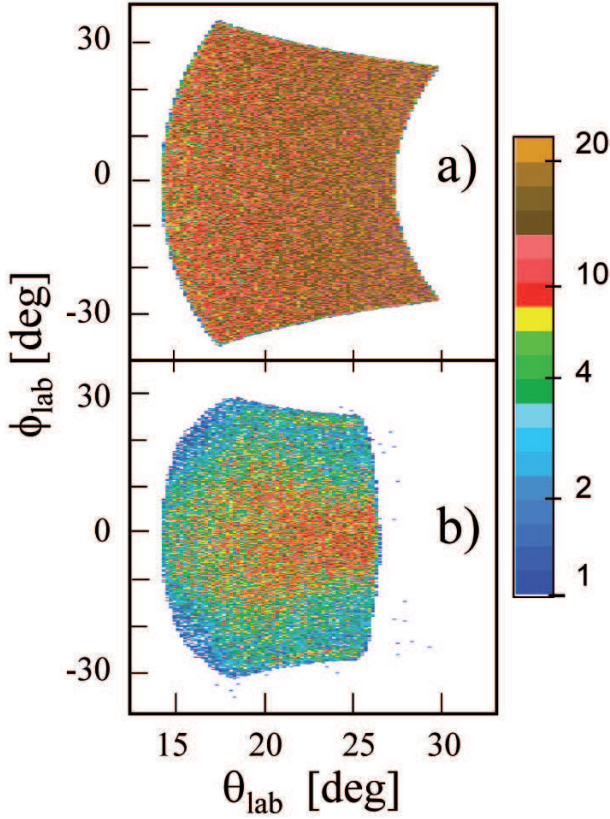
Fig. 3. MCP detector image of the initial distribution for ^{48}Ca ions (a), and the transported distribution obtained with the condition that the incoming ions have reached the focal plane (b). The coincidence requirement results in approximately a factor of two reduction of the statistics and in an inhomogeneous distribution. Here θ_{lab} and ϕ_{lab} are the azimuthal and polar angles, in the laboratory frame, with respect to the beam axis.
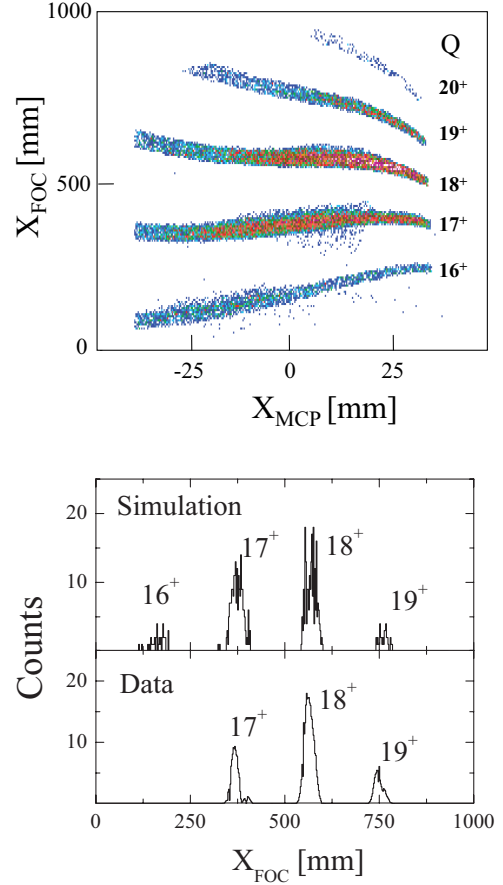

Fig. 4. Upper panel: simulated distribution of charge states of ^{48}Ca with kinetic energy $E_K = 244$ MeV, as a function of the horizontal coordinate of the entrance and focal plane detectors of PRISMA. Lower panel: focal plane distribution of the charge states for $X_{MCP} = 0$ (see text).

of the fragments is kept unmodified after the target. The C-foil of the MCP detector is not taken into account, we estimated that it leads to minor changes at the energies here considered. A complete modelling of the evolution of the charge distribution (involving a correct treatment of the isomeric states) is beyond the scope of this contribution since it is very complex and is system and energy dependent.

The effect of the transmission in the spectrometer can be seen in panel b) of fig. 3, where we show the simulated MCP event distribution requiring the transport of the ions up to the focal plane. It results in a non-uniform distribution of events, more marked at the edge of the acceptance region.

The transmitted yields (integrated over the azimuthal angle ϕ_{lab}) are shown in fig. 5 for the charged states $Q = 16^+, 18^+, 19^+$ (panels a), b), c)) and for the total distribution (panel d)), as a function of the scattering angle (θ_{lab}) and kinetic energy (E_K). For each charge state a non-uniform transport is obtained, although the input

distributions were generated uniform both in energy and angle.

The two-dimensional total distribution enables us to calculate the response function of PRISMA, defined, for each value of energy and angle, as the ratio of the transported events over the initial one. Its inverse provides directly the factor $f(E_K, \theta_{lab})$, shown in fig. 6, needed to correct the experimentally measured yield. As pointed out before, the major corrections are found at the edge of the angular acceptance, with a clear dependence on the kinetic energy of the transported ions.

4 Test of the PRISMA response with calculated cross sections

The effectiveness on the PRISMA response calculated via the illustrated Monte Carlo simulation has been tested by using different initial distributions, but for convenience we decided to use an input distribution corresponding to the differential cross sections calculated with the semiclassical
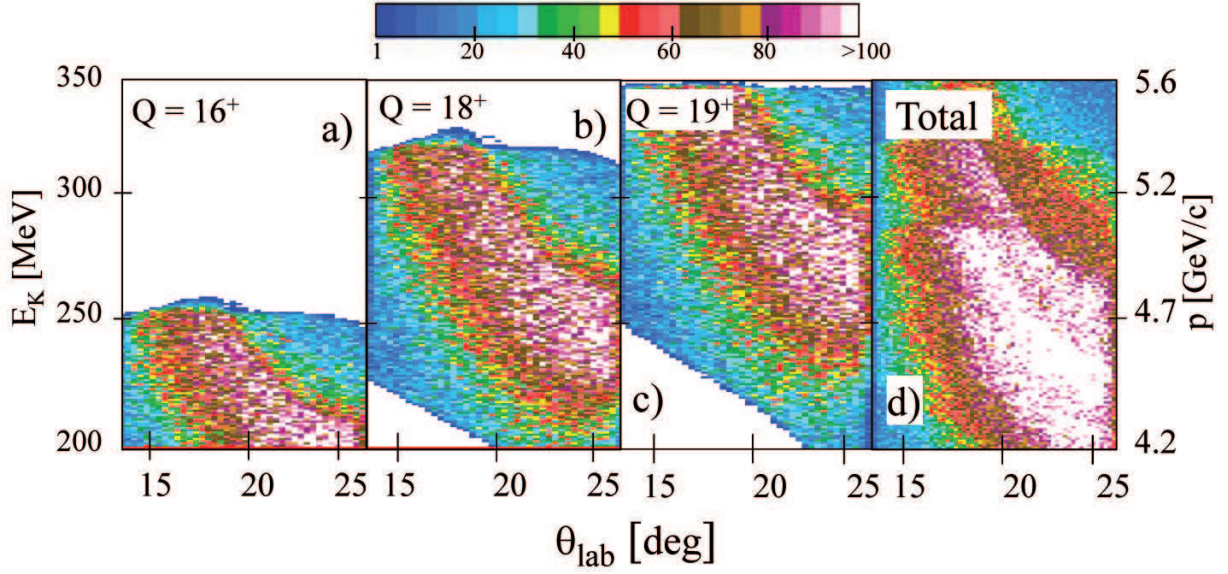
Fig. 5. The transmitted yields for ^{48}Ca ions are shown, as a function of (E_K, θ_{lab}). Panels a), b) and c) refer to the transport of events for each individual charge states $Q = 16^+$, 18^+, 19^+, while panel d) gives the transport of the total charge state distribution (constructed by using five millions events). The momentum scale is given on the right vertical axis.
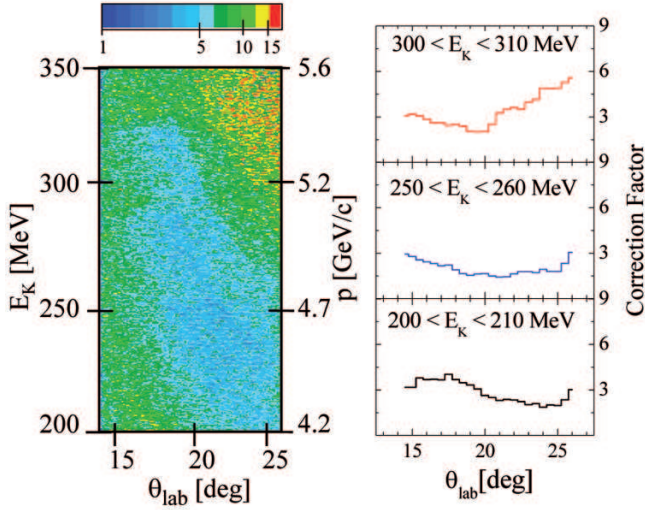

Fig. 6. The correction factor $f(E_K, \theta_{lab})$ for ^{48}Ca ions is shown on the left panel, with the momentum scale on the right vertical axis. Energy cuts of the correction factor are shown on the right.

model GRAZING [7]. This model, from the knowledge of the intrinsic structure of the colliding ions, is able to calculate mass, charge, energy and angular distributions for multinucleon transfer reactions and it has been applied for the analysis of several heavy-ion reactions [16]. The model computes the evolution of the reaction by taking into account, besides the relative motion variables, the intrinsic degrees of freedom of projectile and target. These are the isoscalar surface modes and the single-nucleon transfer channels. The multinucleon transfer channels are described via a multistep mechanism. The relative motion of the system is calculated in a nuclear plus Coulomb

field where for the nuclear part the empirical potential of ref. [17] has been used. The excitation of the intrinsic degrees of freedom is obtained by employing the well-known form factors for the collective surface vibrations and the one-particle transfer channels [18,19]. The model takes into account in a simple way the effect of neutron evaporation.

With GRAZING we have generated double differential cross sections (in angle and energy) for the most prominent final states of the ^{48}Ca on ^{64}Ni reaction at $E_{lab} = 270$ MeV (full line of fig. 7). These inital distributions have been transported to the focal plane of the spectrometer using the ray tracing code outlined above. Integrating in angles or in energy one obtains the energy spectra and the inclusive angular distributions represented by open dots in fig. 7. By applying to the transported events (in the E_K and θ_{lab} plane) the correction factors previously calculated (see fig. 6) one obtains the distributions represented with full dots in the same figure. The corrected distributions agree reasonably well with the ones calculated by GRAZING that have been used as input in our attempt to validate the response function of PRISMA. The fluctuations that are seen in the kinetic energy spectra for some nuclei are due to statistical fluctuations present in the matrix of the correction factor. This matrix has been constructed by using five million events and by adopting a step of 0.1 MeV for the energy and of 0.2 degrees for the scattering angle. In this work we did not implement any smoothing procedure, for instance by adopting a randomization in the bin occupancies, however after a preliminary analysis we could conclude that the statistical fluctuations are important mainly at the edge of the spectrometer where they induce errors of at most 20%.

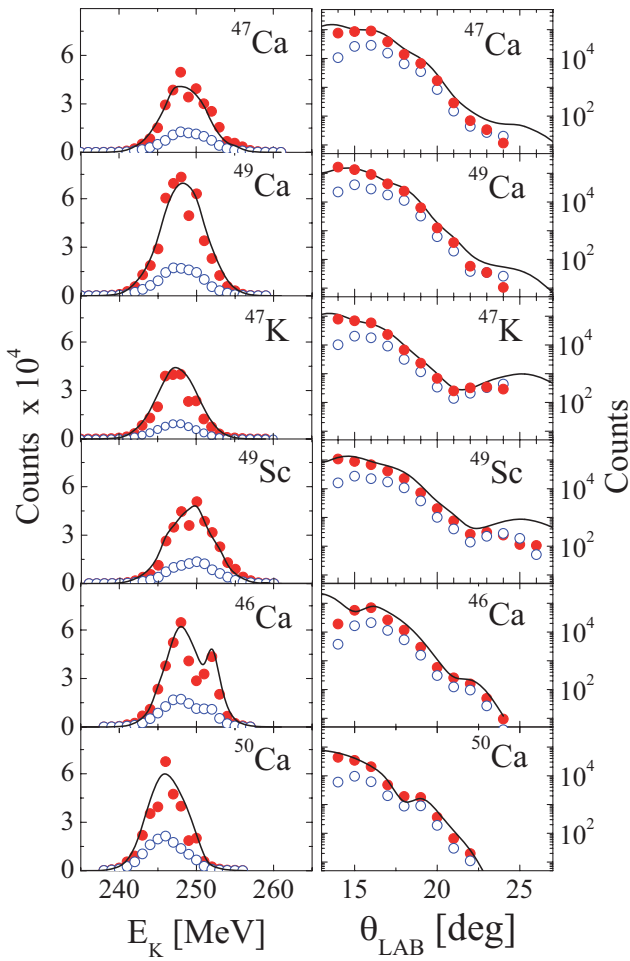The above result gives us confidence that we can now correct the measured distributions for the transmission

Fig. 7. Kinetic energy (left) and dispersion angle θ_{lab} (right) distributions of the $\pm 1n$, $\pm 1p$ $\pm 2n$ channels of the reaction ^{48}Ca on ^{64}Ni at $E_{lab} = 270$ MeV, as calculated by the GRAZ-ING model [7] (solid lines). The open circles give the corresponding simulated distributions obtained at the focal plane of the PRISMA spectrometer, while the full circles represent the same distributions corrected by the factors $f(E_K, \theta_{lab})$, shown in fig. 6 (see text for details).

and thus obtain the actual cross sections for the different final channels. As an example we corrected for the PRISMA transmission the measured angular distributions for the pure elastic and one-neutron stripping channel, shown in fig. 8 in comparison with the semiclassical calculations. The absolute scale of the cross sections has been determined from the elastic scattering as described in ref. [20]. It is found that the reconstructed experimental distributions describe quite well the corresponding distributions of elastic scattering and one-neutron stripping, as a demonstration of the validity of the present method for the analysis of experimental data.

To further illustrate and test the procedure employed for the particle identification that imply the trajectory reconstruction, we have generated with the code GRAZING an initial distribution of events (in energy, angle and mass) for several Ca-like nuclei that are populated in the reac-
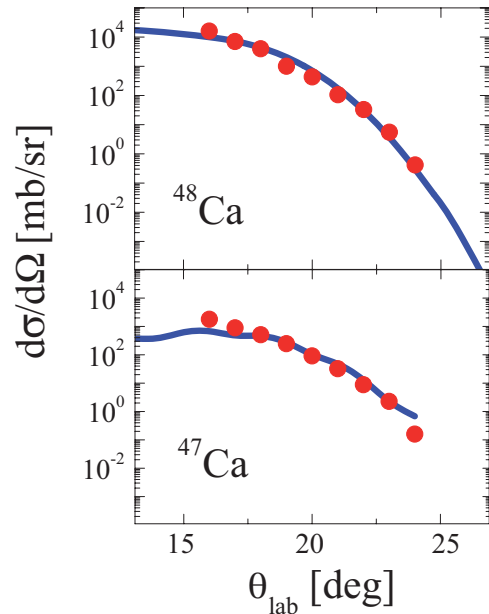

Fig. 8. Angular distributions for the elastic and for the one-neutron stripping channels. Symbols refer to experimental data while solid lines give the theoretical predictions from the semiclassical GRAZING model.
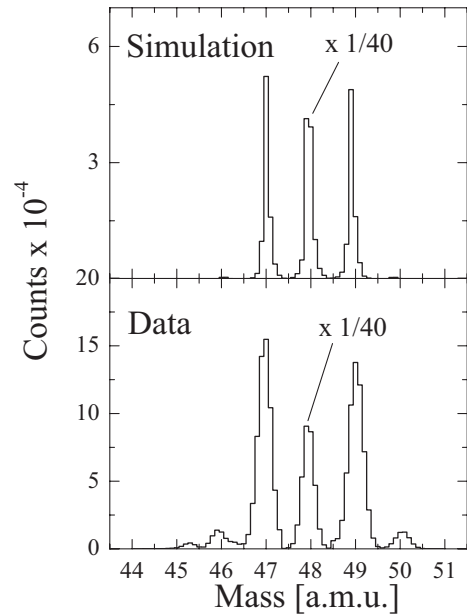

Fig. 9. Experimental and simulated mass spectra for Ca isotopes. In both cases, the ^{48}Ca peak has been reduced by a factor of 40. A mass resolution $\sim 1/150$ and $\sim 1/260$ has been obtained from the experimental and simulated spectra, respectively.

tion. These events are then transported to the focal plane to simulate the experiment. Using the sorting program of the data analysis we obtained the mass spectra shown in fig. 9 in comparison with the experimental ones. In both cases a good mass resolution is obtained ($\sim 1/150$ and $\sim 1/260$ for experiment and simulation, respectively), the simulated spectra having a narrower width mostly due to
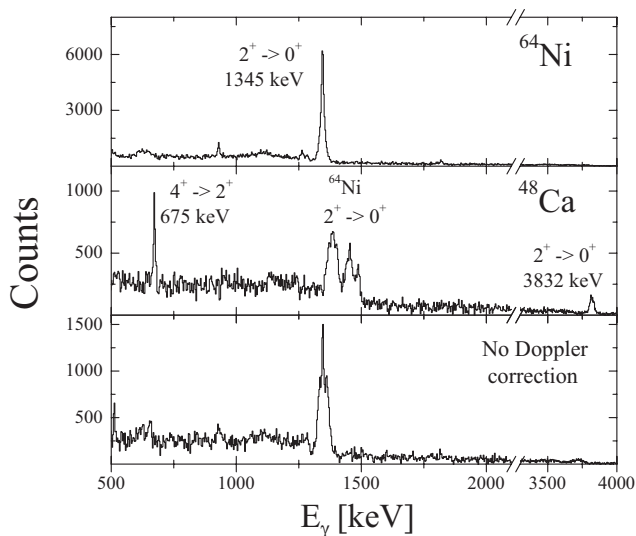
Fig. 10. γ spectra measured in the Ge array CLARA in coincidence with ^{48}Ca ions. The bottom panel shows the experimental data without any Doppler correction, middle and top panels the data obtained applying the Doppler correction for ^{48}Ca (as follows from the trajectory reconstruction) and ^{64}Ni (for the deduced velocity by assuming binary reaction), respectively.

a smaller energy spread and to the fact that one has neglected the finite dimension of the beam spot. The reduction in intensity observed in the simulated two-nucleons transfer channels is a consequence of the underestimate of these channels by the input model.

The fact that the sorting program is able to reconstruct the trajectory with good accurancy is also seen by the experimental γ-ray energy spectra measured by the CLARA array in coincidence with the ions identified with PRISMA. This is visible in fig. 10 where we show the γ-spectra Doppler corrected on event-by-event basis using the velocity and angles provided by the reconstructing sorting code. Even with the rather high velocity of ^{48}Ca ions ($v/c \approx 0.1$), the energy resolution of the $2^+ \to 0^+$ transition at $3.832\,\text{MeV}$ is $\approx 34\,\text{keV}$, which is consistent with the energy uncertainty given by the opening angle of the CLARA Ge crystals.

5 Conclusion

The response function of the PRISMA magnetic spectrometer to the transport of medium mass ions has been studied by a Monte Carlo simulation. The procedure employs a ray tracing code which uses numerical integrators to determine the trajectories of individual rays through the electromagnetic fields. Through the calculated response a non-uniform transmission is found, which is mostly severe at the edge of the angular acceptance of the spectrometer. A test of the calculated response on known input distributions of incoming ions, obtained by a semiclassical model, demonstrates the validity of the present unfolding procedure, which has also been successfully applied to the analysis of experimental data for the same mass region.

References

1. A.M. Stefanini *et al.*, Nucl. Phys. A **701**, 217c (2002).
2. H. Savajols *et al.*, Nucl. Phys. A **654**, 1027c (1999).
3. A. Cunsolo *et al.*, Nucl. Instrum. Methods A **481**, 48 (2002).
4. A. Gadea *et al.*, Eur. Phys. J. A **20**, 193 (2004).
5. D. Bazzacco, Nucl. Phys. A **746**, 248c (2004).
6. S. Pullanhiotan *et al.*, Nucl. Instrum. Methods A **593**, 343 (2008).
7. A. Winther, Nucl. Phys. A **594**, 203 (1995); http://personalpages.to.infn.it/~nanni/grazing/.
8. D. Montanari *et al.*, Acta Phys. Pol. B **40**, 585 (2009).
9. D. Montanari *et al.*, AIP Conf. Proc. **1165**, 386 (2009).
10. G. Montagnoli *et al.*, Nucl. Instrum. Methods **547**, 455 (2005).
11. S. Beghini *et al.*, Nucl. Instrum. Methods **551**, 364 (2005).
12. A. Latina, PhD Thesis, University of Torino (2004).
13. DANFYSIK A/S Web site: http://www.danfysik.dk/.
14. R.O. Sayer, Rev. Phys. Appl. **12**, 1543 (1972).
15. K. Shima *et al.*, Nucl. Instrum. Methods **200**, 605 (1982).
16. L. Corradi *et al.*, J. Phys. G: Nucl. Part. Phys. **36**, 113101 (2009).
17. R.A. Broglia, A. Winther, *Heavy Ion Reactions* (Addison-Wesley Publ. Co., Redwood City, Cal., 1991).
18. R.A. Broglia, G. Pollarolo, A. Winther, Nucl. Phys. A **361**, 307 (1981).
19. G. Pollarolo, R.A. Broglia, A. Winther, Nucl. Phys. A **406**, 369 (1983).
20. S. Szilner *et al.*, Phys. Rev. C **76**, 024604 (2007).